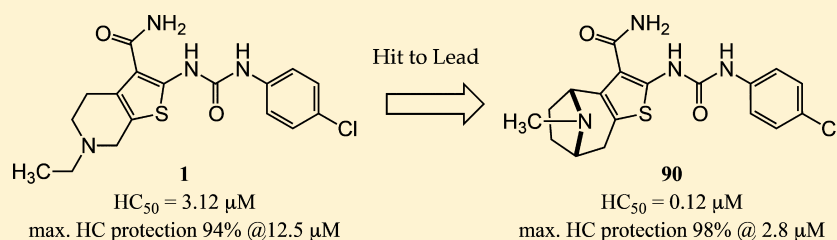


Phenotypic Optimization of Urea–Thiophene Carboxamides To Yield Potent, Well Tolerated, and Orally Active Protective Agents against Aminoglycoside-Induced Hearing Loss

Sarwat Chowdhury,[†] Kelly N. Owens,[‡] R. Jason Herr,[§] Qin Jiang,[§] Xinchao Chen,[§] Graham Johnson,^{||,⊥} Vincent E. Groppi,[#] David W. Raible,^{‡,∇} Edwin W Rubel,[‡] and Julian A. Simon^{*,†,○,¶,||}[†]Clinical Research, [○]Human Biology, and [¶]Public Health Sciences Divisions, Fred Hutchinson Cancer Research Center, Seattle, Washington 98109, United States[‡]Virginia Merrill Bloedel Hearing Research Center, University of Washington, Seattle, Washington 98195, United States[§]AMRI, Albany, New York 12203, United States^{||}NuPharmAdvise LLC, Sanbornton, New Hampshire 03269 United States[⊥]Oricula Therapeutics, Seattle, Washington 98154, United States[#]Center for Discovery of New Molecules, University of Michigan, Ann Arbor, Michigan 48109, United States[∇]Department of Biological Structure, University of Washington, Seattle, Washington 98195, United States

Supporting Information



ABSTRACT: Hearing loss is a major public health concern with no pharmaceutical intervention for hearing protection or restoration. Using zebrafish neuromast hair cells, a robust model for mammalian auditory and vestibular hair cells, we identified a urea–thiophene carboxamide, **1** (ORC-001), as protective against aminoglycoside antibiotic (AGA)-induced hair cell death. The 50% protection (HC₅₀) concentration conferred by **1** is 3.2 μM with protection against 200 μM neomycin approaching 100%. Compound **1** was sufficiently safe and drug-like to validate otoprotection in an *in vivo* rat hearing loss model. We explored the structure–activity relationship (SAR) of this compound series to improve otoprotective potency, improve pharmacokinetic properties and eliminate off-target activity. We present the optimization of **1** to yield **90** (ORC-13661). Compound **90** protects mechanosensory hair cells with HC₅₀ of 120 nM and demonstrates 100% protection in the zebrafish assay and superior physiochemical, pharmacokinetic, and toxicologic properties, as well as complete *in vivo* protection in rats.

INTRODUCTION

Acquired hearing loss can be caused by a variety of environmental and organic factors ranging from noise exposure and pharmaceutical agents to infections, late onset genetic disorders, and aging.^{1,2} Hair cells of the inner ear are the mechanosensors that transduce a physical stimulus, vibrations transmitted by the fluid-filled compartment of the cochlea and vestibule, into nerve impulses that are converted in the central nervous system into the perception of sound and vestibular reflexes. Most forms of hearing loss are sensorineural in nature, meaning they result from death or injury of the cochlear hair cells or other cell types in the organ of Corti of the cochlea or the neurons connecting the hair cells to the brain.³ Unlike aquatic vertebrates and birds, mammals lack the ability to regenerate hair cells making hearing loss irreversible.^{4,5} The mechanisms by which hair cells are killed are complex and

overlapping. Elements of programmed cell death, or apoptosis, as well as necrotic signatures have been identified in damaged hair cells *in vitro* and *in vivo*.^{5–8} Antioxidants including aspirin, *N*-acetyl cysteine (NAC), and selenium compounds⁹ have been reported to offer some degree of protection in model organisms^{3,10} but have yielded disappointing results in human clinical trials.^{11–13} Mechanistically, stress pathways, including the *c*-Jun N-terminal kinase (JNK), mixed lineage kinase (MLK), and p38 kinase pathways, have been implicated in drug-induced ototoxicity, and small molecule inhibitors of these pathways have been proposed as protective agents.^{8,14–17} However, clinical trials have again been disappointing, possibly because the protection is not robust and falls off at higher doses

Received: June 23, 2017

Published: October 9, 2017

of the ototoxic agent.¹⁸ These clinical findings indicate a need for better therapeutic agents effective at higher doses of ototoxic agent.

Aminoglycoside antibiotics (AGAs) constitute a class of natural product antibiotics that are effective against a variety of clinically important Gram-negative bacteria.¹¹ However, because of side effects that include irreversible hearing and balance problems (ototoxicity) and kidney damage (nephrotoxicity), their use is limited in North America and Western Europe to combating life-threatening infections.^{19–21} Exceptions are the use of systemic AGAs for controlling flare-ups of chronic *Pseudomonas aeruginosa* infections in cystic fibrosis patients and multidrug resistant tuberculosis.^{22–25} AGAs exert their antimicrobial effect partly by binding to rRNA and altering or inhibiting ribosomal protein synthesis.^{26–29} A more controversial model of toxicity in bacterial and mammalian cells through direct induction of reactive oxygen species (ROS) has been proposed but remains hotly contested.^{30–32} Additionally, proteins that bind AGAs have been identified and proposed as relevant mediators of *in vivo* ototoxicity.³³

In an unbiased approach, we used the lateral line neuromast hair cells in free-swimming larval zebrafish (*Danio rerio*) to screen for compounds that protect these mechanosensory hair cells against AGA-induced cell death.³⁴ Like mammalian auditory and vestibular hair cells, lateral line hair cells transduce a mechanical stimulus of changing liquid pressure to nerve impulses and, like their auditory counterparts, are exquisitely sensitive to damage or death due to AGA exposure. Neuromast hair cell toxicity can be used as a highly reliable and versatile screening assay to identify modifiers, either enhancers or suppressors, of ototoxic agents.³⁴ The assay is equally effective in identifying genetic and pharmacological modifiers. In a screen of structurally diverse, small molecule, drug-like compounds, we identified a thiophene–urea carboxamide **1** (ORC-001, PROTO-1, Figure 1),²⁰ as an agent that provided

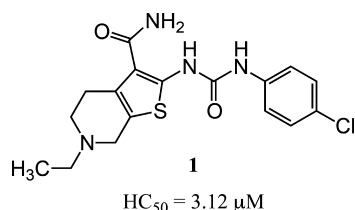


Figure 1. Structure of **1**.

dose-dependent protective activity (otoprotection) against a range of AGA concentrations. Further experiments revealed that **1** was sufficiently drug-like to allow proof-of-concept testing in a rat model of AGA-induced hearing loss (see below). However, **1** exhibited pharmacokinetic and toxicological liabilities including only adequate solubility, moderate oral bioavailability, short *in vivo* half-life, and moderate inhibition of

the human ether-à-go-go-related gene (hERG, aka $K_{V11.1}$) potassium ion channel. Inhibition of hERG by a diverse array of pharmaceuticals has been linked to cardiac arrhythmias through QT interval prolongation.^{35–38} Because of this, hERG inhibition is generally viewed as a liability in drug development. Finally, as a hit in a phenotypic screen, **1** was uncharacterized in terms of its molecular target or mechanism of action.^{39,40} To overcome these limitations, we carried out a systematic evaluation of analogs using a phenotypic hair cell protection assay in zebrafish to generate a structure–activity relationship for compounds that protect against aminoglycoside antibiotic-induced hearing loss. The results of this evaluation and validation of hearing protection in mammals by one of the final lead compounds are the subjects of the current manuscript.

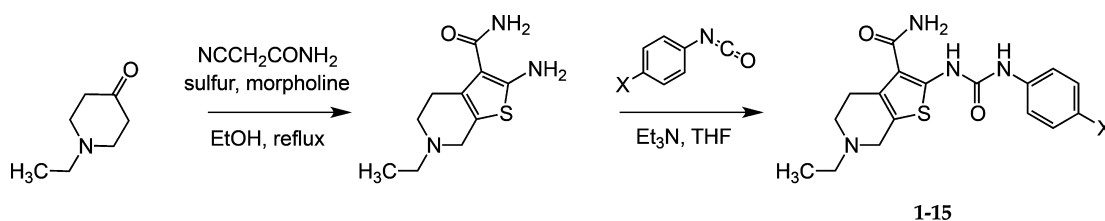
RESULTS

Synthesis of 1- and 3-Aryl Urea Derivatives. In a phenotypic screen using zebrafish neuromast hair cells, we identified **1** as highly protective against aminoglycoside antibiotic-induced hair cell death. Early ADME characterization revealed several promising properties as a lead molecule (adequate aqueous solubility and membrane permeability, reasonable plasma protein binding, no issues with CYP stability or inhibition, and an acceptable clearance profile), although we identified several pharmacokinetic limitations and a hERG liability (hERG IC_{50} 3.26 μ M). However, **1** was sufficiently safe and drug-like to be used to validate otoprotection in an *in vivo* rat model of aminoglycoside-induced hearing loss as a measure of proof of concept (*vide infra*). We then explored the structure–activity relationships of this compound series with three goals in mind: improve otoprotective potency, improve pharmacokinetic properties, and eliminate or minimize off-target activity.

The preparation of **1** and N3'-aryl derivatives began with the Gewald condensation^{41,42} of 4-ethyl-4-piperidone with cyanoacetamide in the presence of elemental sulfur and morpholine to produce 2-amino-4,5,6,7-tetrahydrothieno[2,3-*c*]pyridine-3-carboxamide **28** as shown in Scheme 1. Subsequent reaction of **28** with aryl isocyanates produced the urea derivatives **1–15** in moderate to good yields. Formation of HCl salts stabilized compounds containing a basic nitrogen in the tetrahydropyridine ring and related structures, which otherwise slowly underwent aereal oxidation to generate fluorescent conjugated products that interfered in the primary bioassay. In all, over 400 analogues including amines and quaternary ammonium salts were prepared and evaluated in the zebrafish neuromast hair cell protection assay.

In Vivo Screen of 1 Analogs in Zebrafish. New compounds were tested in the zebrafish assay as previously described.^{34,43} In summary, newly hatched free-swimming AB zebrafish larvae were raised at 28.5 °C in Petri dishes and transferred to cell culture baskets lined in 6-well culture plates

Scheme 1. Gewald Reaction To Form 2-Amino-thiophene Carboxamides



in groups of ten fish per basket. Fish were pretreated with test compound for 1 h at five 3-fold dilutions followed by treatment with 200 μM neomycin. Following neomycin exposure, fish were rinsed briefly with a staining agent (DASPEI), anesthetized, and mounted on the stage of an epifluorescence dissecting microscope. Hair cell staining of ten neuromasts on one side of each animal was evaluated visually, and each neuromast was scored for presence of a normal complement of hair cells, with reduced or absent DASPEI staining indicating a reduction in hair cell number. Composite scores were calculated for animals in each treatment group, normalized to the control group and expressed as % hair cell survival. If hair cell survival was at least 50%, the HC_{50} was calculated. These data are shown in Tables 1–8 and representative dose response

Table 1. Protective Activity of Urea Variants in the Zebrafish Hair Cell Protection Assay^a

	R	HC_{50} (μM)
1		3.12
2		3.13
3		1.62
4		11.5
5		17.4
6		1.78
7		3.39
8		2.91
9		13.0
10		10.3
11		NA
12		NA
13		NA
14		NA
15		NA

^aNA indicates not active ($\text{HC}_{50} > 25 \mu\text{M}$).

relationship experiments for several analogues in the zebrafish hair cell protection assay are shown in Figures 2 and 3. All zebrafish protocols were approved by the University of Washington IACUC.

Structure–Activity Relationship (SAR). For the purposes of the determination of structure–activity relationships, 1 was conceptualized as composed of six structural units: (1) N3-aryl

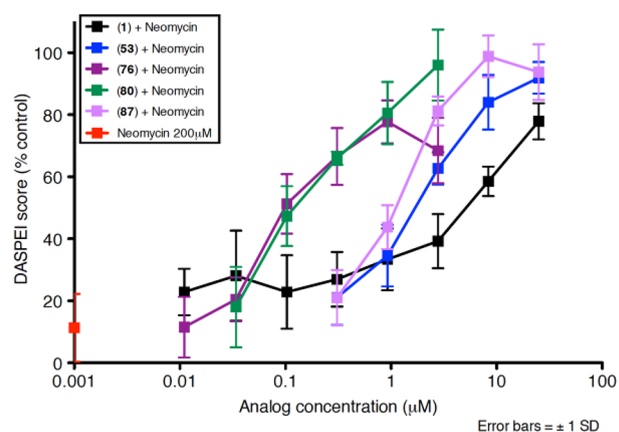


Figure 2. Dose–response functions for zebrafish neuromast hair cells treated with neomycin (200 μM) plus 1, 53, 76, 80, or 87 or neomycin alone.

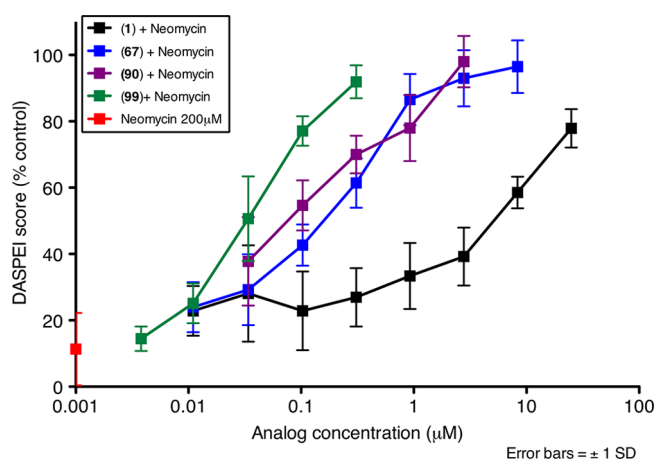


Figure 3. Dose–response functions for zebrafish neuromast hair cells treated with neomycin (200 μM) plus 1, 67, 90, or 99 or neomycin alone.

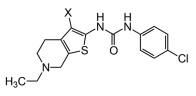
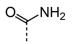
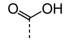
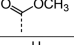
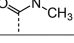
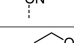
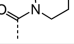
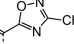
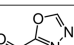
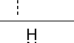
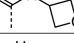
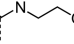
substituents on the urea; (2) the 1,3-disubstituted urea; (3) thiophene core; (4) primary carboxamide C2 substitution; (5) tetrahydropyridine core; and (6) *N*-ethyl group. The goal of the SAR-determining studies described here was 3-fold: first, to determine the contribution of each structural element described above to the observed biological activity; second, to improve the protective activity of the compound series; and third, to improve the pharmacokinetic and toxicological properties of the lead compounds. A systematic variation of each structural element and its effect on protective activity is described.

The examination of the effects of N3-substitution to replace the *p*-chlorophenyl group relied on the reaction of readily synthesized isocyanates or their equivalents with 2-aminothiophene-3-carboxamide 28. A variety of aromatic and nonaromatic isocyanates gave rise to a panel of substituted ureas as shown in Table 1. The pattern of activity was indicative of a narrow range of allowable substituents with *p*-chlorophenyl being close to optimal. Several aryl ureas had comparable protective activity to 1 ($\text{HC}_{50} = 3.12 \mu\text{M}$), such as the classic isosteric replacements at the C4 position (2, 3, 7, and 8, $\text{HC}_{50} = 1.6\text{--}3.4 \mu\text{M}$ range). Interestingly, the unsubstituted analog 14 was inactive, and the bioisosteric 3,4-disubstituted pair 5 and 6 differed in potency by 10-fold ($\text{HC}_{50} = 1.78$ vs 17.4 μM for 5), reinforcing the narrow requirement for allowable

substitution. The “extended” benzyl analogues represented by **11** were inactive, as were *N*-alkyl derivatives, represented by **12** and **13**, clearly lying out of the tolerable substitution range. Heterocyclic derivative **15** was similarly inactive, as were the majority of the 2-substituted aromatic analogues (data not shown).

As shown in Table 2, replacement of the primary carboxamide with a carboxylic acid **16**, methyl ester **17**, *N*-

Table 2. Protective Activity of Carboxamide Variants in the Zebrafish Hair Cell Protection Assay^a

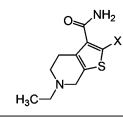
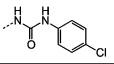
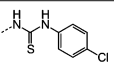
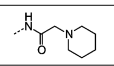
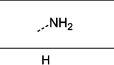
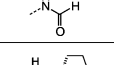
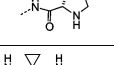
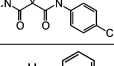
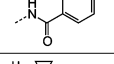
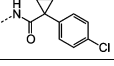
	X	HC ₅₀ (μM)
1		3.12
16		NA
17		NA
18		NA
19		NA
20		NA
21		NA
22		NA
23		NA
24		9.40
25		9.38

^aNA indicates not active (HC₅₀ > 25 μM).

methyl amide **18**, carbonitrile **19**, and tertiary amide **20** greatly reduces the activity, suggesting that both protons on the primary amide are required for activity. Similarly, carboxamide bioisosteric compounds 1,2,5-oxadiazole **21** and 1,3,4-oxadiazole **22** are inactive. Only the 2-hydroxyethyl carboxamide **24** and 2-(*N*-morpholino)ethyl carboxamide **25** retain modest activity (both HC₅₀ = 9.4 μM), suggesting the possibility that an internal hydrogen bond with the proximal urea proton may provide a preorganization of molecular structure that contributes to compound potency.

As shown in Table 3, efforts to replace the disubstituted urea moiety were largely unsuccessful, although the disubstituted thiourea **26** did provide modest potency, albeit 2-fold less (HC₅₀ = 6.57 versus 3.12 μM). Replacement of urea with several types of amide structures resulted in no protective activity in **27**, **29**, **30**, **32**, or **33**, and unsurprisingly the core compound **28** without a disubstituted urea functional group was inactive. Cyclopropyl malonamide **31** displayed a lack of potency, and likewise substitution at either the urea N1 or N3 position was also not tolerated (data not shown). Replacement of the disubstituted urea with a peptide bond or a squarate diamide also completely abolished protective activity (data not shown).

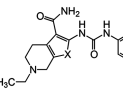
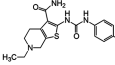
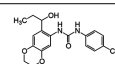
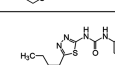
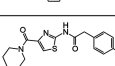
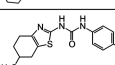
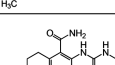
Table 3. Protective Activity of 2-Aminothiophene Variants in the Zebrafish Hair Cell Protection Assay^a

	X	HC ₅₀ (μM)
1		3.12
26		6.57
27		NA
28		NA
29		NA
30		NA
31		NA
32		NA
33		NA

^aNA indicates not active (HC₅₀ > 25 μM).

The thiophene portion of the core fused bicyclic ring is also important for activity (Table 4). Several 5- and 6-membered

Table 4. Protective Activity of Thiophene Variants in the Zebrafish Hair Cell Protection Assay^a

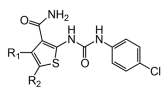
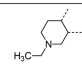
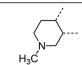
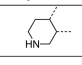
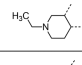
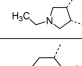
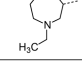
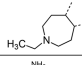
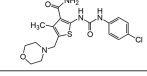
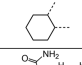
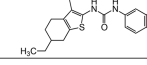
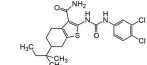
	X	HC ₅₀ (μM)
1		3.12
34		NA
35		NA
36		NA
37		NA
38		NA

^aNA indicates not active (HC₅₀ > 25 μM).

ring thiophene variants were prepared from commercial building blocks to give **34**–**37**, none of which provided protective activity. The biosisosteric tetrahydroisoquinoline **38** was also prepared but likewise displayed no potency in the bioassay.

The variation of the parent tetrahydrothieno[2,3-*c*]pyridine ring proved feasible without eliminating biological activity, with protective activity remaining in the 1–5 μM range (Table 5).

Table 5. Protective Activity of Tetrahydropyridine Variants in the Zebrafish Hair Cell Protection Assay^a

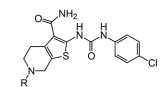
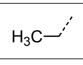
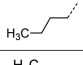
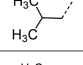
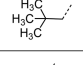
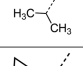
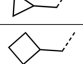
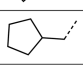
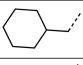
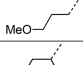
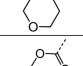
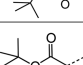
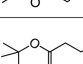
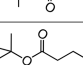
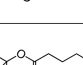
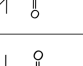
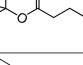
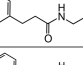
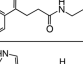
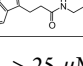
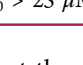
	R ₁ /R ₂	HC ₅₀ (μM)
1		3.12
39		4.70
40		3.26
41		4.61
42		4.34
43		3.98
44		5.80
45		6.92
46		NA
47		NA
48		NA

^aNA indicates not active (HC₅₀ > 25 μM).

Movement of the nitrogen to produce tetrahydrothieno[3,2-*c*]pyridine **41** was tolerated (HC₅₀ = 4.61 μM), as was ring-contraction to the dihydrothieno[2,3-*c*]pyrrole **42** (HC₅₀ = 4.34 μM) and ring-expansion to the tetrahydrothienoazepines **43** and **44** (HC₅₀ = 3.98 and 5.80 μM, respectively). However, replacement of the tetrahydropyridine ring with the carbocyclic cyclohexanes **46–48** completely abolished protective activity. Breaking up the fused bicyclic core to provide the tertiary aminomethyl tetra-substituted thiophene **45** provided a compound of moderate but measurable activity (HC₅₀ = 6.92 μM).

Interestingly, removal of the *N*-ethyl substituent as in **40** had only a modest effect on activity (HC₅₀ = 3.26 μM for **40** versus 3.12 μM for **1**), leading to an exploration of the effect of *N*-substitution on potency, as shown in Table 6. A series of *N*-alkyl hydrocarbon analogues **49–58** were prepared to provide a simple exploration of changes in length and steric bulk. While the increase in bulk at the terminal end of the linear case reduced activity (*N*-ethyl **1**, HC₅₀ = 3.12 μM, to *N*-isobutyl **50**, HC₅₀ = 4.51 μM, to *N*-neopentyl **51**, HC₅₀ = 5.56 μM, to *N*-isopropyl **52**, HC₅₀ = 1.49 μM), a few alkyl substituents bearing terminal cyclic motifs led to improved additional improvements in protective activity [*N*-(cyclopropyl)ethyl **53**, HC₅₀ = 1.22 μM, to *N*-(cyclobutyl)ethyl **54**, HC₅₀ = 1.36 μM, to *N*-(cyclopentyl)ethyl **55**, HC₅₀ = 1.83 μM, to *N*-(cyclohexyl)methyl **56**, HC₅₀ = 1.89 μM, versus 3.12 μM for **1**]. Unfortunately, along with increases in hearing protection potency, a number of compounds in this same set also exhibited increases in hERG activity as determined by the patch clamp assay (hERG IC₅₀ = 2.67 μM for **53** and 0.73 μM for **54**

Table 6. Protective Activity of Tetrahydropyridine *N*-Alkyl Variants in the Zebrafish Hair Cell Protection Assay^a

	R	HC ₅₀ (μM)
1		3.12
49		3.50
50		4.51
51		5.56
52		1.49
53		1.22
54		1.36
55		1.83
56		1.89
57		2.40
58		2.83
59		NA
60		NA
61		1.10
62		0.56
63		0.71
64		0.62
65		0.47
66		0.11
67		0.10

^aNA indicates not active (HC₅₀ > 25 μM).

versus 3.26 μM for **1**). To test the effect of amine basicity on potency, carbamate **59** and aminoethyl ester **60** were prepared, with the result that protective activity was completely suppressed. Interestingly, as the hydrocarbon chain connecting the trialkylamine to the ester functionality was increased to two carbons to give **61**, potency was increased (HC₅₀ = 1.10 μM for **61** versus 3.12 μM for **1**). When the length was increased between three and five methylene units in **62–64**, the potency was improved to less than a micromolar activity (HC₅₀ = 0.6–0.7 μM range). Unlike the hydrocarbon substituent series, however, the increases in potency were not necessarily paralleled by their hERG inhibition, (hERG IC₅₀ = 3.84 μM for **62** versus 3.26 μM for **1**). Compounds incorporating an amide functionality distal to the tetrahydropyridine nitrogen as

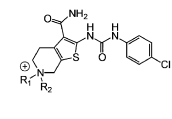
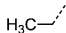
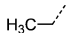
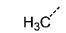


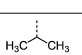

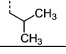
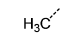
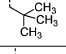
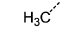
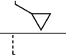
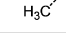
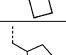
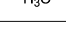
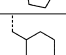


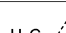
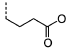
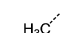
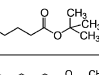
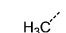
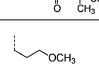
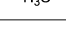
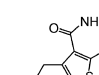

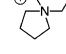

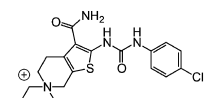
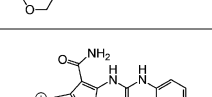
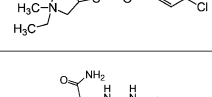
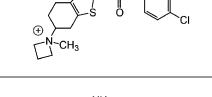
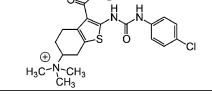
in **65**–**67** also retained improved protective activity, providing some of the most potent compounds prepared in the *N*-alkyl SAR series (HC_{50} = 0.1–0.5 μ M range).

In order to more fully explore the requirement for a basic nitrogen in the tetrahydropyridine ring, we synthesized a panel of *N,N*-dialkyl quaternary ammonium salts (Table 7). This provides a permanent positive charge within the ring, whereas the previous compounds were assumed to be protonated at physiological pH. The initial *N*-methyl analogue **68** was found to be slightly more potent than the parent compound (HC_{50} = 1.96 μ M for **68** versus 3.12 μ M for **1**), but interestingly it exhibited the same level of hERG inhibition (hERG IC_{50} = 3.38 μ M for **68** versus 3.26 μ M for **1**). We were initially pleased to find that increasing steric bulk around the nitrogen yielded compounds with increasing activity (*N*-ethyl **68**, HC_{50} = 1.96 μ M, to *N*-isobutyl **71**, HC_{50} = 0.38 μ M, to *N*-neopentyl **72**, HC_{50} = 0.29 μ M), although a limit was reached with *N*-isopropyl compound **70** (HC_{50} = 0.96 μ M). Similarly, increasing the size of a cyclic moiety on the terminal end of the *N*-substituent led to increasingly more potent compounds [*N*-(cyclopropyl)ethyl **73**, HC_{50} = 0.36 μ M, to *N*-(cyclobutyl)ethyl **74**, HC_{50} = 0.21 μ M, to *N*-(cyclopentyl)ethyl **75**, HC_{50} = 0.20 μ M, to *N*-(cyclohexyl)methyl **76**, HC_{50} = 0.10 μ M]. It was therefore a pleasant discovery that the hERG activity decreased inversely from that observed in the *N*-alkyl series. For instance, interaction with the hERG channel decreased as the zebrafish potency increased for the size increase from the *N*-ethyl compound **68** (HC_{50} = 1.96 μ M, hERG IC_{50} = 3.38 μ M) to *N*-isobutyl compound **71** (HC_{50} = 0.38 μ M, hERG IC_{50} = 9.75 μ M) to *N*-(cyclohexyl)methyl compound **76** (HC_{50} = 0.10 μ M, hERG IC_{50} > 30 μ M). As with the basic *N*-substituted variants in Table 6, quaternary ammonium salts containing methyl ether and ester functional groups tethered by increasing length aliphatic linkers yielded highly active compounds **78**–**81** shown in Table 7.

A number of other quaternary ammonium congeners were prepared as more significant scaffold modifications (Table 7). Spirocyclic pyrrolidine-dihydrothieno[2,3-*c*]pyridinium compound **82** and spirocyclic morpholine-dihydrothieno[2,3-*c*]pyridinium compound **83** were both more potent than the *N*-ethyl-*N*-methyl parent compound (HC_{50} = 0.41 μ M for **82** and HC_{50} = 1.21 μ M for **83** versus HC_{50} = 1.96 μ M for **68**), but the former displayed the same level of hERG inhibition (IC_{50} = 3.51 μ M for **82** versus IC_{50} = 3.38 μ M for **68**), whereas the latter compound displayed only moderate hERG activity (IC_{50} = 12.4 μ M for **83**). The quaternary dihydrothieno[2,3-*c*]pyrrole analogue **84** was similar to the parent tetrahydrothieno[2,3-*c*]pyridine **68** both in terms of hearing protection (HC_{50} = 3.10 μ M for **84**) and hERG inhibition (IC_{50} = 3.29 μ M for **84**). Two compounds in which the quaternary ammonium functional group was outside of the fused bicyclic ring system were prepared, but both were less active (HC_{50} = 3.92 μ M for **85** and HC_{50} = 5.87 μ M for **86**).

The steric environment around the basic tetrahydropyridine nitrogen was further explored by the synthesis of the 2,2,6,6-tetramethyl tetrahydropyridine derivative **87** (Table 8), which was prepared from tetramethyl piperidone through the route depicted in Scheme 1. This compound was more active than the parent compound (HC_{50} = 1.24 μ M for **87** versus HC_{50} = 3.12 μ M for **1**), but more importantly it was devoid of hERG liability (IC_{50} > 30 μ M for **87** versus IC_{50} = 3.26 μ M for **1**). In vitro ADME profiling of **87** demonstrated that it had excellent metabolic stability and no issues with CYP inhibition but

Table 7. Protective Activity of Quaternary Ammonium Salt Derivatives in the Zebrafish Hair Cell Protection Assay

	R ₁	R ₂	HC ₅₀ (μ M)
1		n/a	3.12
68			1.96
69			0.45
70			0.96
71			0.38
72			0.29
73			0.36
74			0.21
75			0.20
76			0.10
77			0.10
78			0.25
79			0.14
80			0.11
81			0.48
82			0.41
83			1.21
84			3.10
85			3.92
86			5.87

suffered from poor aqueous solubility (13 μ M) and modestly increased plasma protein binding (96.5% in human and 95.8% in rat plasma).

Table 8. Protective Activity of Bicyclic Tetrahydropyridine (Tropane) Analogues in the Zebrafish Hair Cell Protection Assay

Compound	R	HC ₅₀ (μM)
1		3.12
87		1.24
89		2.25
90		0.12
92		7.21
93		0.27
95		3.92
96		0.27
98		5.00
99		0.03

In an effort to evaluate the importance of conformational flexibility of the tetrahydropyridine unit, we set out to synthesize the bicyclic, tropane-like compound **91** as a racemate (Figure 5). The standard Gewald sequence using commercially available tropinone to react with cyanoacetamide and elemental sulfur in the presence of base yielded a mixture with two predominant products, each having the correct molecular weight of the desired product as well as ¹H NMR spectra consistent with the expected product structure. An admixture of the two yielded distinct but partially overlapping NMR spectra suggesting that the two did not interconvert under these conditions. The 2-aminothiophene materials were difficult to purify and fully characterize and instead were reacted as a mixture with *p*-chlorophenyl isocyanate to give a mixture of racemic regioisomers **88** and **91** (Figure 5). Again, both

compounds exhibited mass and ¹H NMR spectra consistent with the expected product. Both compounds had good protective activity with **88** slightly more active than **91** [HC₅₀ = 0.36 μM for **88** versus HC₅₀ = 0.83 μM for **91**]. The expected product contains two asymmetric centers at the bridgehead carbon atoms and would be produced as a racemate. The more active of the two racemic compounds **88** was resolved by chiral HPLC chromatography to yield the individual enantiomers as **89** and **90** (ORC-13661).⁴⁴ The structural ambiguity of the products derived from the original tropinone–Gewald reaction was eventually resolved by determining the single crystal X-ray diffraction structure of **90** HCl salt as shown in Figure 4 (Supporting Information, Figure S2 and S3 and Table S2). Surprisingly, the synthesis of **90** resulted from a previously undescribed alternate reaction pathway in the Gewald condensation, resulting in a reversed regiochemistry of the thiophene relative to the bicyclic tropinone starting material.

The crystal structure unambiguously proves the absolute structure of **90** as (1*R*,8*S*)-4-[[[(4-chlorophenyl)carbamoyl]-amino]-11-methyl-5-thia-11-azatricyclo[6.2.1.0^{2,6}]undeca-2-(6),3-diene-3-carboxamide hydrochloride. Based on this the crystal structure, we assigned the structures of **89**, **90**, **92**, and **93** as shown in Figure 5, with **91**, **92**, and **93** representing the “expected” Gewald products. The mechanism of the “unexpected” Gewald reaction to yield **88**, **89**, and **90** is under investigation. An alternate synthetic approach starting from chiral (+)-2-tropinone was developed subsequently and provided **90** that was identical by mass spectrometry, ¹H NMR spectroscopy, and chiral HPLC as the material derived from achiral 3-tropinone. The asymmetric synthesis of **90** will be the subject of a subsequent publication.

Protection assays in zebrafish revealed that **90** is the more potent enantiomer (HC₅₀ = 0.12 μM), while **89** is considerably less effective (HC₅₀ > 2.25 μM). The eudismic ratio (ER) of 18.8 suggests that **90** interacts with a chiral target. The less potent racemate **91** was also resolved by chiral HPLC to provide the individual enantiomers as **92** and **93**. The levorotatory enantiomer **93** is more potent (HC₅₀ = 0.27 μM) while the dextrorotatory enantiomer **92** is considerably less active (HC₅₀ = 7.21 μM, ER 26.7). Reaction of the *N*-BOC tropinone under standard Gewald conditions followed by *p*-chlorophenyl-urea formation yielded a single product **94** (Figure 5), albeit in poor yield, that was carried through *N*-BOC removal and chiral resolution to yield the *N*-H compounds **95** and **96**. Based on ¹H NMR chemical shift of the diagnostic C-6 (X-ray structure numbering) methine proton, we assigned the structures of **94**, **95**, and **96** as shown (Figure 5). As with the *N*-methyl compounds **92** and **93**, the levorotatory *N*-H enantiomer **96** was more potent (HC₅₀ = 0.27 μM) while the dextrorotatory enantiomer **95** was less active (HC₅₀ = 3.92 μM, ER 14.7), lending additional support to our structural assignments. Completing the *N*-H and *N*-methyl regiochemical tropane-fused thiophene sets, we

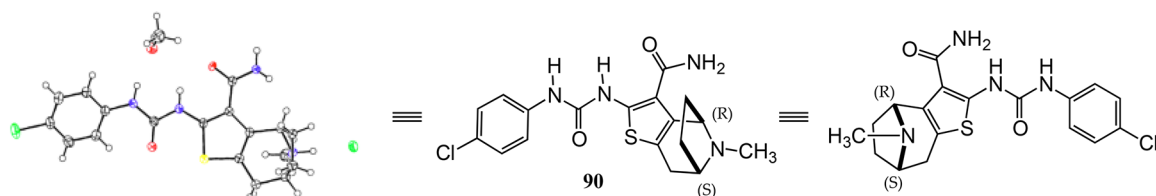


Figure 4. Crystal structure of **90**.

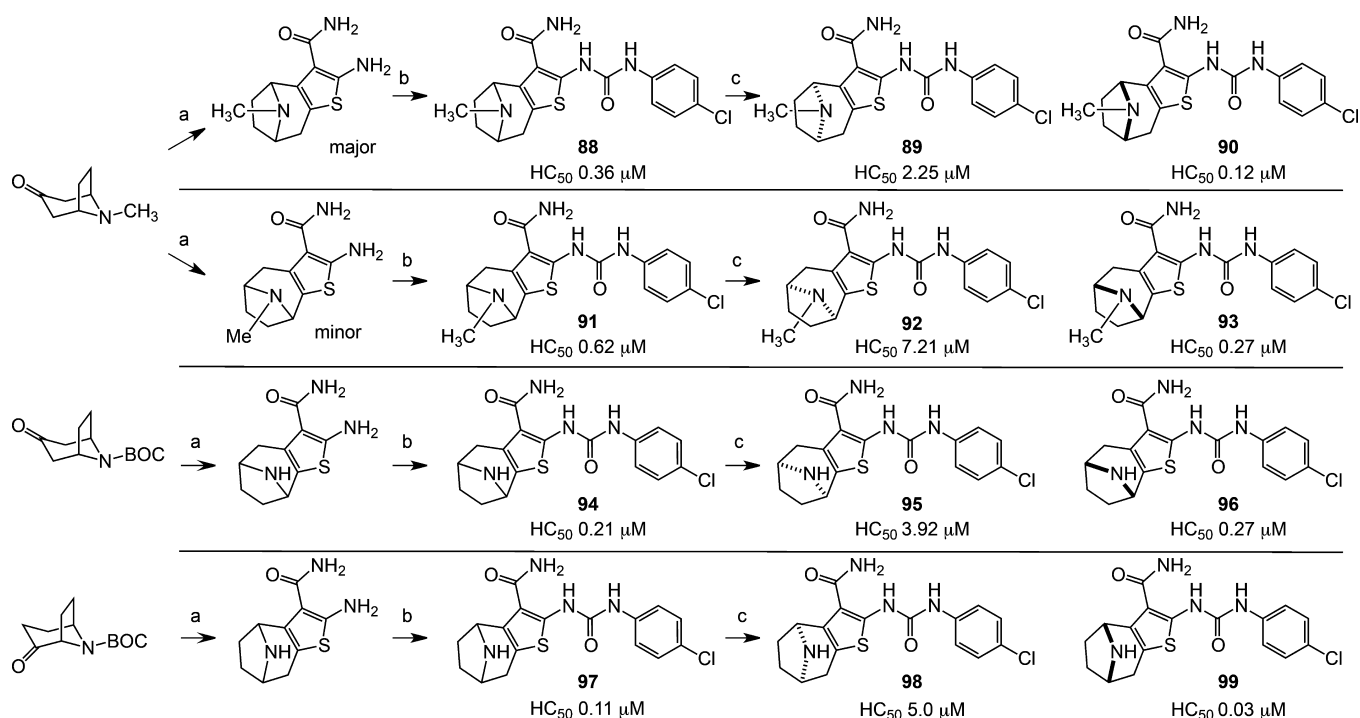


Figure 5. Synthesis and resolution of chiral tropane analogues: (a) $NCCH_2CO_2Et$, S_8 , morpholine, EtOH; (b) $p\text{-ClC}_6\text{H}_4\text{N}=\text{C}=\text{O}$, TEA, THF; (c) chiral HPLC separation.

reacted racemic N-BOC 2-tropinone under the Gewald conditions to afford racemic **97**. Chiral HPLC separation of **97** could only be accomplished prior to N-BOC group deprotection. Subsequent removal of the N-BOC group yielded enantiomers **98** and **99**.

Examination of the structural relationship among the active enantiomers of the two thiophene orientation Gewald products for the N-methyl **90** and **93** and N-H compounds **96** and **99** reveals a similar relationship to that seen with the regioisomeric tetrahydropyridines **1** and **41** (Table 5). Altering the position of the basic nitrogen relative to the thiophene ring while maintaining the overall scaffold geometry yields compounds with similar biological activity. The tropinone compounds **90**, **93**, **96**, and **99** exhibit superior protective activity with HC_{50} in the 33–270 nM range while their corresponding enantiomers **89**, **92**, **95**, and **98** have significantly reduced activity. Based on activity and accessibility, indole-containing N-alkyl derivative **67** (Table 6), 2,2,6,6-tetramethyl tetrahydropyridine derivative **87** (Table 8), and **90** were selected for early preclinical characterization along with **1** (Figure 1).

Preclinical Characterization of **1**, **67**, **87**, and **90**.

Although the hit-to-lead phase of the campaign resulted in several very potent and efficacious derivatives of **1**, the triage of compounds using the early ADME results was the determining factor in deciding which analogues to take forward for early pharmacokinetic evaluation. As a number of the quaternary ammonium salt compounds were not orally bioavailable and also found to inhibit the hERG channel, we elected to focus on the tertiary amine derivatives. As a result, we chose to profile three compounds, in addition to **1** (HC_{50} = 3.12 μ M): the terminal indole-containing N-alkyl compound **67** (Table 6, HC_{50} = 0.10 μ M), the 2,2,6,6-tetramethyl tetrahydropyridine derivative **87** (Table 8, HC_{50} = 1.24 μ M), and the bicyclic tropane-like compound **90** (Table 8, HC_{50} = 0.12 μ M). Therefore, the pharmacokinetic, metabolic, and *in vitro*

toxicological properties for these candidates were determined. The compounds have moderate to good aqueous solubility [85 μ M for **1**, 86 μ M for **67**, 83 μ M for **87**, and 76 μ M for **90** for the free base forms], acceptable plasma protein binding profiles [95.9% (human) and 94.1% (rat) **1**, 99.9% (human) and 99.9% (rat) for **67**, 96.5% (human) and 95.8% (rat) for **87**, and 90.7% (human) and 90.1% (rat) for **90**], and elimination kinetics with half-lives of 2.1 h for **1**, 7.1 h for **67**, 6.2 h for **87**, and 7.8 h for **90**. Compounds **1**, **87**, and **90** exhibited no *in vitro* toxicity against the HepG2 cell line (IC_{50} > 300 μ M), whereas compound **67** inhibited growth of HepG2 cells with IC_{50} 17 μ M. All four compounds were well tolerated in an acute toxicity assay in rats at 50 mg/kg iv. As noted, hit compound **1** inhibited the hERG ion channel (hERG IC_{50} = 3.26 μ M) giving a ratio of 1.2 (hERG/ HC_{50}). On the other hand, compounds **67**, **87**, and **90** were less potent hERG inhibitors with IC_{50} values of 20.1 μ M, >30 μ M, and 5.6 μ M, respectively, and with hERG/ HC_{50} ratios of 201, >24, and 47, respectively. In addition to hERG inhibition, **1** was found to gradually undergo partial air oxidation to yield an inactive, highly fluorescent byproduct. Compound **67** was shown to have marginal oral bioavailability (>1%), while **1**, **87**, and **90** had acceptable to good oral bioavailability (46%, 21%, and >50%). Compounds **87** and **90** are resistant to the oxidation pathway observed for **1** (as well as **67**) by virtue of geminal dimethyl substitution in **87** and the bicyclic tropane framework of **90**.

Compounds **1** and **90** were tested for *in vitro* and *in vivo* interference with aminoglycoside antimicrobial activity. There was no interference by either drug with neomycin minimal inhibitory concentration (MIC) or minimal bactericidal concentration (MBC) against *E. coli* ATCC25922. Additionally, **90** exhibited no interference in the MIC for tobramycin, amikacin, kanamycin and neomycin against five strains of *P. aeruginosa* or amikacin MIC against *M. tuberculosis*. Finally, **90** showed no interference in an *in vivo* mouse pulmonary

tuberculosis model with amikacin, kanamycin, and moxifloxacin (see Supporting Information, Table S4-1 and S4-2).

In Vivo Testing of ORC Compounds in Rats. On the basis of early preclinical evaluation, compounds **1** and **90** were tested in an *in vivo* rat model of aminoglycoside-induced hearing loss. The auditory brain stem response (ABR) assay is a widely used, noninvasive method for quantification of auditory function in vertebrates, including humans. Male Sprague–Dawley rats 5–7 weeks old were purchased from Harlan Laboratories. Briefly, rats are anesthetized and placed in a sound-attenuated enclosure on a heating pad to maintain body temperature at 37.5 °C. Electrical responses from the ear and CNS are detected with subcutaneous needle electrodes. Positive and negative electrodes are inserted at the left temporal bone above the pinna and at the vertex of the skull, with the ground electrode in the thigh. Free-field pure-tone stimuli are generated by custom software and presented as short (5 ms) acoustic pulses with 1 ms rise/fall times at a repetition rate of 19/s. In addition, broadband clicks are presented at the beginning and end of each session to assess any changes in the animal's condition. Neural responses are amplified, bandpass filtered (100–3000 Hz), digitized using custom software, and displayed online as an average response to the repeated acoustic stimulus. A sequence of pure tone stimuli of varying frequencies (2, 4, 8, 16, and 32 kHz) and intensities (usually 15–90 dB, SPL) is presented, and the resulting waveforms are recorded. All individual responses and averaged responses were saved. Examination of the averaged sound-induced waveforms by a trained experimenter yields the hearing thresholds (minimum sound level required to induce a reliable waveform at each frequency tested).

In preliminary experiments, we showed that **1** injected intravenously (*iv*) was nontoxic to rats at doses up to 25 mg/kg. This dose also yielded a plasma half-life of 1.7 h. Based on literature precedent, we carried out *in vivo* hearing protection experiments using kanamycin (500 mg/(kg·day) *sc*). The results of these experiments are shown in Figure 6. After initial ABR testing, male Sprague–Dawley rats 50–60 days old were treated with kanamycin 500 mg/(kg·day) (*sc*) for 14 days and then allowed to recover without treatment for an additional 2 weeks before final ABR testing. A second group was subjected to the same treatment with the addition of exposure to **1** at 25 mg/(kg·day) by intraperitoneal injection. Control groups included animals receiving **1** alone, the vehicle for **1** (Cremaphor EL/DMSO/EtOH/PBS) alone, or no treatment. ABR testing (Figure 6) reveals a highly significant hearing loss at 8–32 kHz that is greatest at the higher frequencies in animals treated with kanamycin alone. This hearing loss was completely prevented by **1** at 8 and 16 kHz and mostly resolved at the highest frequency tested (32 kHz). All rat protocols were approved by the University of Washington IACUC.

We selected compound **90** as our lead compound for full preclinical evaluation based on its superior protective activity in the zebrafish assay, decreased hERG-inhibitory activity, and superior pharmacokinetic properties (Figure 7 and Supporting Information, Table S1) and efficiency of large scale synthesis. Compound **90** was tested for *in vivo* protection using amikacin, a more widely employed aminoglycoside antibiotic than kanamycin in the clinic. For testing the *in vivo* mammalian efficacy of **90**, we used Fischer 344 rats 7–9 weeks old at the time of testing, purchased from Taconic. Rats were exposed to amikacin alone at 320 mg/(kg·day) (*sc*) for 12 days or the same amikacin exposure plus **90** (5 mg/(kg·day), *po*) for the

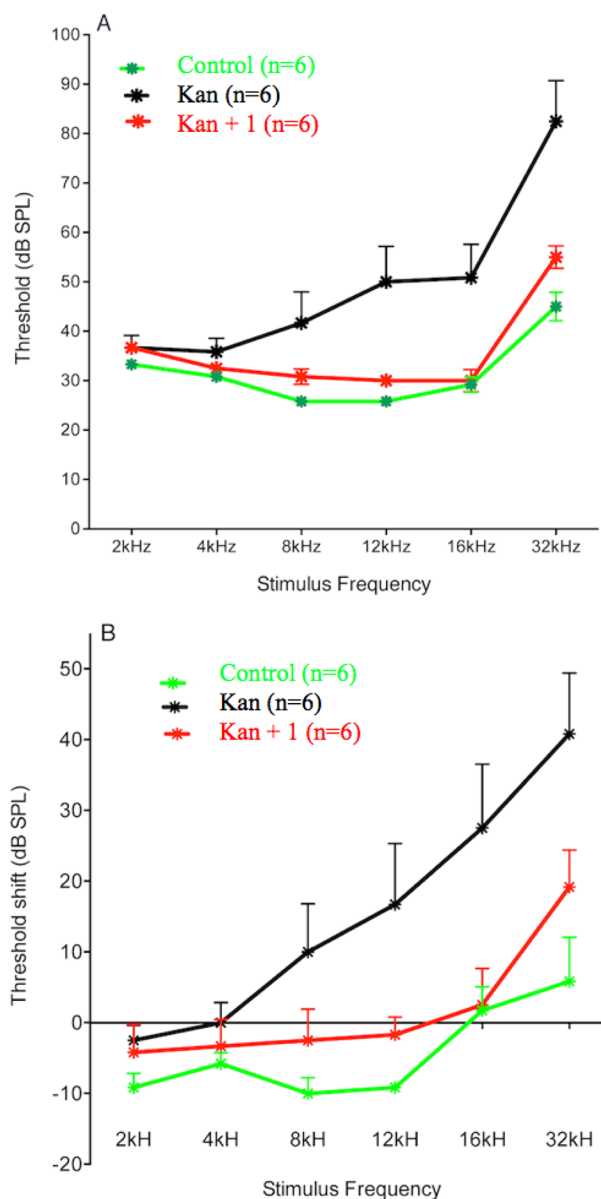


Figure 6. Protection of hearing in Sprague–Dawley rats treated with kanamycin for 14 days (500 mg/(kg·day) *sc*) by concurrent *ip* administration of **1** (25 mg/(kg·day)). (A) Mean (+1 SEM) ABR thresholds in rats recorded an additional 14 days after the 14-day drug treatment with **1** alone, kanamycin, or coadministration with kanamycin and **1**. (B) Mean (+1 SEM) threshold shifts in hearing from pretreatment levels 14 days after the treatment for each group. Positive values indicate increasing levels of hearing loss.

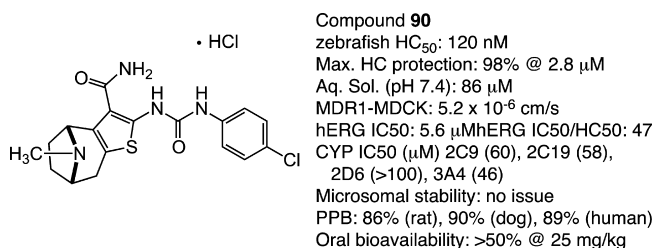


Figure 7. ADME profiling for compound **90**.

same period. Additional rats were treated with **90** alone (5 mg/(kg·day) [*n* = 3], or 25 mg/(kg·day) [*n* = 3], *po*) for 12 days.

In all experiments **90** was delivered by oral gavage. We find that exposure to amikacin compared to kanamycin causes significantly more reproducible hearing loss in animals treated with AGA alone. For oral gavage, the vehicle for **90** was PEG300/DMA/EtOH/H₂O. ABR thresholds were determined for each rat prior to drug treatment. Rats were then treated with amikacin alone or amikacin plus **90** daily for 12 days and then allowed to recover for 2 weeks before final ABR testing. As shown in Figure 8, Fischer 344 rats treated with amikacin (320

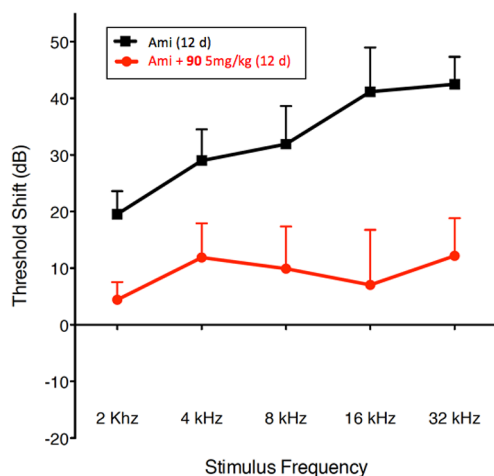


Figure 8. Protection of hearing in Fischer 344 rats treated with amikacin (320 mg/(kg·day) sc) for 12 days with or without concurrent oral administration of **90** (5 mg/(kg·day)). Threshold shift from pretreatment hearing levels at 2-weeks following treatment period.

mg/(kg·day) sc) alone for 12 days exhibited moderate to severe hearing loss at all frequencies tested. Co-administration of amikacin (320 mg/(kg·day) sc) and **90** (5 mg/(kg·day) po) for 12 days resulted in highly significant hearing protection across all frequencies tested. Furthermore, the resulting average hearing thresholds of this group are well within the normal range, and 6 of the 8 rats tested in this group showed complete protection from hearing loss due to the aminoglycoside exposure. None of the rats treated with **90** alone showed reliable changes in hearing thresholds (data not shown). In support of the audiological findings, immunohistochemical examination of the inner and outer hair cells of the organ of

Corti from experimental animals showed significant disruption of normal tissue architecture (Figure 9, panel A) in Fischer 344 rats treated with amikacin alone (Figure 9, panel B). The amikacin-induced hair cell death in the organ of Corti was suppressed by cotreatment with **90**.

DISCUSSION

Protection of hearing through pharmacological intervention against the myriad insults that are capable of causing hearing loss has been a long sought-after goal.⁴⁵ We describe the development and preclinical characterization of a family of urea–thiophene carboxamides culminating in **90**, an orally active and well tolerated agent with excellent pharmacokinetic and metabolic properties. Compound **90** protects rat hearing against amikacin-induced ototoxicity while showing no effect on *in vitro* or *in vivo* antibacterial activity of several clinically relevant AGAs. Our structure–activity relationship (SAR) for this compound series is based on over 300 analogs interrogating all elements of the core structure of the screening hit **1**.³⁴ Our studies identified structural elements that are absolutely required for protective activity as well as those that can be substantially altered without disrupting the biological activity. The *p*-chlorophenyl urea substituent appears to be optimal as a wide variety of substituted aryl urea compounds exhibit comparable activity at best. Significant changes of the aryl substituent nature or position lead to loss of activity. The bis-monosubstituted urea is absolutely required for activity as even modest change such as replacement by an amide or cyclopropyl malonamide or *N*-methylation abolishes activity. Likewise, the thiophene-3-carboxamide is critical for protective activity as replacement of either thiophene or carboxamide with even conservative structural variants leads to dramatic loss of activity.

The *N*-ethyl tetrahydropyridine moiety of **1** provided the richest ground for structural variation. A basic nitrogen or quaternary ammonium salt is needed for activity, presumably existing in a mostly or completely cationic state at physiological pH for favorable electrostatic interactions with its target. The positive charge can however reside at the tetrahydropyridine 2-position (as in **1**) or 3-position (as in **41**, Table 5), in a 5-membered ring (as in **42**, Table 5) or 7-membered ring (as in **43** and **44**, respectively, Table 5), or as part of a rigid bicyclo-[3.2.1]-aza-octane (tropane) ring system (as in **90** and **93**,

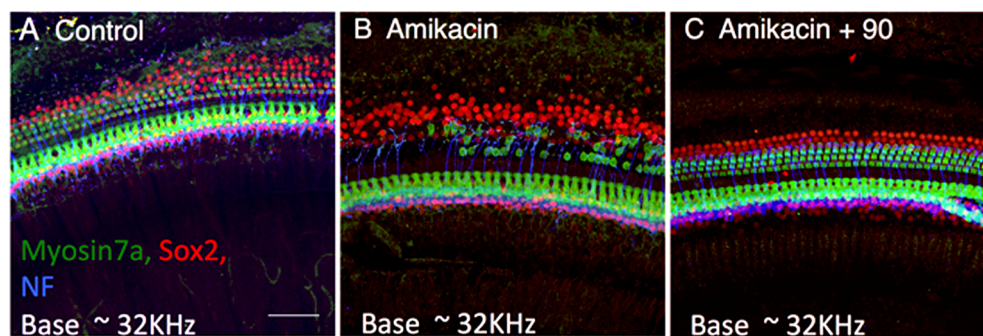


Figure 9. Confocal images of the organ of Corti basal turn: representative examples from each treatment group. (A) control, saline treated, sc daily for 12 days; (B) amikacin treated, sc daily, 320 mg/(kg·day) for 12 days; (C) amikacin (Ami) + **90**, amikacin sc daily, 320 mg/(kg·day), + **90** po daily, 5 mg/kg, for 12 days. Cochleae from animals were fixed with 4% paraformaldehyde and dissected. Organs of Corti were incubated with cell-type specific antibodies: antimyosin 7A antibody (hair cells, green), anti-Sox2 antibody (supporting cell nuclei, red) and anti-neurofilament (NF) antibody (neuronal processes, blue). All animals were treated with drug for 12 days. Final post-treatment ABR testing was done after an additional 12 day period. Animals euthanized after ABR testing for histological examination.

Table 8). Extending the *N*-alkyl substituent to 2-naphthyl- or indole-containing amides (as in **66** and **67**, Table 6) yielded the most active compounds in the zebrafish assays but at the cost of physicochemical properties. Compound **67** has the high potency value ($HC_{50} = 70$ nM) but lacks solubility and oral bioavailability making it unsuitable for *in vivo* testing in the rat. Based on the high potency of aryl amide analogs like **67**, we investigated the possibility of appending functional groups that would be useful for mechanistic and target identification studies. We discovered that a wide range of substituents are tolerated when connected to the tetrahydropyridine nitrogen through a 7- to 17-atom linker. Analogs containing a fluorescent probe (i.e., BODIPY), as well as an affinity tag (i.e., biotin), have been synthesized based on the existing SAR and are currently being used in mechanistic and target identification efforts. Among the most active ORC compounds in this series are **90** ($HC_{50} = 120$ nM), **93** ($HC_{50} = 270$ nM), **96** ($HC_{50} = 270$ nM) and **99** ($HC_{50} = 33$ nM), which vary only in *N*-substitution on the 8-azabicyclo[3.2.1] ring system and position of the 2-carbon bridge relative to the thiophene ring (Figure 5). Because of its superior potency in the zebrafish hair cell protection assay and improved pharmacokinetic properties, **90** was advanced through IND-enabling studies under the auspices of Oricula Therapeutics.

CONCLUSION

In the absence of a molecular target, elaboration of our original screening hit **1**, into a full SAR program was made possible using the phenotypic zebrafish neuromast hair cell viability assay to predict *in vivo* activity in a mammalian model. This effort yielded **90** as a promising clinical candidate for the prevention of aminoglycoside induced hearing loss in patients. Clinical adoption of such an agent would reinvigorate the safe use of this underused broad class of effective antibiotics and thus expand their utility in the treatment of serious and life-threatening bacterial infections.

EXPERIMENTAL SECTION

Zebrafish Neuromast Hair Cell Protection Assay. Adult AB zebrafish were bred and newly fertilized embryos were collected the week prior to testing and raised at 28.5 °C in Petri dishes containing embryo medium (1 mM $MgSO_4$, 0.15 mM KH_2PO_4 , 50 μM Na_2HPO_4 , 1 mM $CaCl_2$, 500 μM KCl, 115 mM NaCl, 700 μM $NaHCO_3$). Newly hatched free-swimming larvae were fed paramecia at 4 days postfertilization (dpf). All procedures were approved by the University of Washington Animal Care and Use Committee. For initial efficacy testing of each new experimental compound, fish 5–7 dpf were transferred to cell culture baskets placed in 6-well culture plates containing 7 mL of embryo medium. Typically, tests are done with ten fish per basket but work well with up to 50 fish. All treatment and wash volumes are 7 mL. Fish were pretreated with test compound for 1 h at five initial concentrations (1.56, 3.125, 6.25, 12.5, and 25 μM). Following this exposure to the test compound alone, fish were moved to a new well containing the test compound plus 200 μM neomycin (neomycin sulfate, Sigma, St. Louis, MO, catalog no. N1142) for 1 h. If significant hair cell protection was observed at the lowest concentration, the dosages were reduced by half until hair cell protection was eliminated. All experimental compounds were tested alongside the following controls groups: fish treated with neomycin (200 μM) alone; fish treated with test compound (25 μM) alone; fish treated with **1** at the same concentration range as test compound; and untreated fish using the same procedures.

Following neomycin exposure, fish were rinsed briefly 4 times in embryo medium and 700 μL of 0.05% DASPEI (2-{4-(dimethylamino)styryl}-*N*-ethylpyridinium iodide, Molecular Probes,

Eugene, OR) was added and allowed to stain for 15 min. DASPEI brightly labels the hair cells of each neuromast due to their robust packing in mitochondria.⁴⁶ Following this labeling and two rinses in embryo medium, the fish were anesthetized with 350 μL of MS222 (0.55 $\mu g/mL$ final concentration, 3-aminobenzoic acid ethyl ester, methanesulfonate salt, Sigma, St. Louis, MO).

For assessment of the dose–response protective functions, the fish in each experimental and control group were transferred to separate wide depression slides in embryo medium with MS222. Slides were mounted on the stage of an epifluorescence dissecting microscope equipped with a DAPSEI filter set (excitation 450–490 nM and barrier 515 nM, Chroma Technologies, Brattleboro, VT). The hair cell staining of ten neuromasts (SO1, SO2, IO1, IO2, IO3, IO4, M2, MI1, MI2, and O2) on one side of each animal was visually evaluated.⁴⁷ Each neuromast was scored for presence of a normal complement of hair cells (score = 2), reduced DASPEI staining indicating a reduction in hair cell number (score = 1), or absence of DASPEI staining (score = 0). The total score for each animal was tabulated to give a composite score that ranged from 0 to 20 for each fish. Average scores and standard deviations were calculated for animals in each treatment group. Scores were normalized to the control group (vehicle only, no drug, no neomycin) and expressed as % hair cell survival. If hair cell survival was at least 50%, the 50% effective concentration (HC_{50}) was calculated as a linear extrapolation from the nearest concentrations of protective drug that produced hair cell survival below and above 50%.

Rat Auditory Brain Stem Response (ABR) Assay for Hearing Protection. Male Fischer 344 rats were purchased from Harlan Laboratories (Livermore CA) at 40–50 days postnatal. Auditory brainstem responses (ABRs) were measured from each rat twice, once 1–2 weeks prior to drug treatments and again at 2 weeks after the termination of drug treatment. Rats were anesthetized with isoflurane, placed on a heating pad to maintain body temperature near 37 °C, and placed in a sound-attenuating chamber. AB responses were recorded using standard subcutaneous needle electrodes with the positive and negative electrodes at the left temporal bone above the pinna and the vertex of the skull, and the ground electrode in the thigh. Free-field pure tone stimuli were generated, and ABR recordings were digitized using custom software. Tone pips were 5 ms in duration with 1 ms rise/fall times, presented at a repetition rate of 19/s. In addition, broadband clicks were presented at the beginning and end of each session to assess for any changes in the animal's condition. All stimuli were calibrated online at the beginning of each experiment with a calibrated probe microphone. Neural responses were preamplified (100 \times ; A-M Systems amplifier model 3000), sent through an MA3 amplifier with an additional 20 dB post-preamp gain (Tucker Davis Technologies), bandpass filtered (100–3000 Hz; Krohn-Hite filter model 3550), and digitized at 24.4 kHz. We sampled responses in a 15 ms window (with a 5 ms stimulus onset delay). The threshold was defined as the lowest sound pressure level (SPL) in which a recognizable waveform was present and repeatable. Thresholds were determined at 2, 4, 8, 16, and 32 kHz and for a broad-band click. Stimuli were presented 500 times from 80 to 20 dB SPL in steps of 10 and then 1000 repetitions in steps of 5 dB SPL when approaching threshold. Near threshold each series was repeated to determine the reliability of the waveform at the estimated threshold, 5 dB above and 10 dB below the estimated threshold. When animals appeared to be deaf at a particular frequency, the stimulus was presented at the maximum intensity generated by our system (90–100 dB) SPL at least twice at 1000 repetitions to be assured of a complete hearing loss. The threshold was then arbitrarily set at 100 dB SPL. All averaged responses were examined online, and thresholds were estimated. Following the experimental session, all responses were printed and rescored twice, once by the experimenter and once by an ABR expert who was blinded with regard to the experimental condition. Threshold estimates were within 5 dB in over 97% of the response traces, and the few that differed by >10 dB were re-examined by the two evaluators to come to a consensus. Data were analyzed as raw thresholds at each test frequency and as “Threshold Shift”, comparing pretest threshold with post-drug-administration threshold, where a positive number indicates a hearing loss (in dB) due to the drug treatment.

Chemistry. All reactions were performed under a dry atmosphere of nitrogen unless otherwise specified. Indicated reaction temperatures refer to the reaction bath, while room temperature (rt) is noted as 25 °C. Commercial grade reagents and anhydrous solvents were used as received from vendors, and no attempts were made to purify or dry these components further. Removal of solvents under reduced pressure was accomplished with a Buchi rotary evaporator at approximately 28 mmHg pressure using a Teflon-linked KNF vacuum pump. Thin layer chromatography was performed using either 1 in. × 3 in. AnalTech No. 02521 or Merck 60 F254 silica gel plates with fluorescent indicator using appropriate solvent mixtures. Visualization of TLC plates was made by observation with either short wave UV light (254 nm lamp) or 10% phosphomolybdic acid in ethanol or in iodine vapors. Medium pressure flash column chromatography was carried out using either a Teledyne Isco CombiFlash Companion Unit with RediSep Rf silica gel columns or a Biotage Isolera with SiliCycle HP cartridges. Proton NMR spectra were obtained either on 300 MHz Bruker Nuclear Magnetic Resonance Spectrometer or 500 MHz Bruker Nuclear Magnetic Resonance Spectrometer, and chemical shifts (δ) are reported in parts per million (ppm), and coupling constant (J) values are given in hertz, with the following spectral pattern designations: s, singlet; d, doublet; t, triplet; q, quartet; dd, doublet of doublets; m, multiplet; br, broad singlet; sym, symmetrical. Tetramethylsilane (TMS) was used as an internal reference. Melting points are uncorrected and were obtained using a MEL-TEMP Electrothermal melting point apparatus. Mass spectroscopic analyses were performed either using positive mode electron spray ionization (ESI) on a Varian ProStar LC-MS with a 1200L quadrupole mass spectrometer or using positive mode atmospheric pressure chemical ionization (APCI) on a Shimadzu LC-MS system. High performance liquid chromatography (HPLC) purity analysis was conducted using a Varian Pro Star HPLC system with a binary solvent system A and B using a gradient elution [A, H₂O with 0.1% trifluoroacetic acid (TFA); B, CH₃CN with 0.1% TFA] and flow rate = 1 mL/min, with UV detection at 254 nm. All final compounds were purified to $\geq 95\%$ purity, and these purity levels were measured by a Varian Pro Star HPLC system. Three different Varian Pro Star HPLC methods were used to establish compound purity. HPLC Method A: Phenomenex Luna C18(2) column (4.6 mm × 250 mm); mobile phase, A = H₂O with 0.1% TFA and B = CH₃CN with 0.1% TFA; gradient 10–95% B (0.0–10 min; hold for 6 min); UV detection at 254 nm. HPLC Method B: SunFire C18 column (4.6 mm × 250 mm); mobile phase, A = H₂O with 0.1% TFA and B = CH₃CN with 0.1% TFA; gradient 10–100% B (0.0–20 min; hold for 5 min); UV detection at 254 nm. HPLC Method C: SunFire C18 column (4.6 mm × 250 mm); mobile phase, A = H₂O with 0.1% TFA and B = CH₃CN with 0.1% TFA; gradient 0–100% B (0.0–15 min; hold for 5 min); UV detection at 254 nm.

2-Amino-6-ethyl-4,5,6,7-tetrahydrothieno[2,3-c]pyridine-3-carboxamide. A stirred mixture of *N*-ethyl-4-pyrrolidinone (22.7 g, 178 mmol), 2-cyanoacetamide (16.5 g, 197 mmol), sulfur (6.87 g, 215 mmol), and morpholine (31.5 g, 362 mmol) in ethanol (350 mL) was heated to reflux under nitrogen for 5 h. After this time, the reaction mixture was cooled to room temperature and concentrated under reduced pressure. The residue was mixed with saturated aqueous sodium bicarbonate (200 mL) and water (200 mL). The aqueous mixture was extracted with methylene chloride (5 × 200 mL). The combined organic extracts were dried over anhydrous sodium sulfate, filtered, and concentrated under reduced pressure. The resulting residue was triturated with cold methanol (30 mL) and filtered. The filter cake was washed with cold methanol (2 × 10 mL) and then dried under reduced pressure to provide the product as a yellow solid (21.7 g, 54%): ¹H NMR (300 MHz, DMSO-*d*₆) δ 6.98 (s, 2H), 6.52 (bs, 2H), 3.29 (s, 2H), 2.66 (d, J = 4.8 Hz, 2H), 2.60 (d, J = 4.8 Hz, 2H), 2.46 (q, J = 7.2 Hz, 2H), 1.04 (t, J = 7.2 Hz, 3H); LRMS m/z 226 [M + H]⁺.

2-[3-(4-Chlorophenyl)ureido]-6-ethyl-4,5,6,7-tetrahydrothieno[2,3-c]pyridine-3-carboxamide (1). To the stirred solution of 2-amino-6-ethyl-4,5,6,7-tetrahydrothieno[2,3-c]pyridine-3-carboxamide (450 mg, 2.00 mmol) in anhydrous tetrahydrofuran (10 mL) at room

temperature under nitrogen was added a solution of 4-chlorophenyl isocyanate (400 mg, 2.40 mmol) in anhydrous methylene chloride (6 mL) dropwise over 3 min. Then the reaction mixture was stirred overnight at room temperature. The reaction mixture was filtered. The filter cake was washed with methylene chloride (5 mL) and then dried under reduced pressure to provide the product **1** (free base) as a white solid (301 mg, 38%): ¹H NMR (300 MHz, DMSO-*d*₆) δ 10.94 (s, 1H), 10.12 (s, 1H), 7.52–7.45 (m, 4H), 7.34 (d, J = 9.0 Hz, 2H), 3.45 (s, 2H), 2.77 (d, J = 4.8 Hz, 2H), 2.65 (d, J = 4.8 Hz, 2H), 2.55–2.45 (m, 2H), 1.07 (t, J = 6.6 Hz, 3H); LRMS m/z 379 [M + H]⁺.

2-[3-(4-Chlorophenyl)ureido]-6-ethyl-4,5,6,7-tetrahydrothieno[2,3-c]pyridine-3-carboxamide Hydrochloride (1 HCl). To the stirred mixture of compound **1** (free base) (157 mg, 0.400 mmol) in methylene chloride (50 mL) at room temperature was added hydrochloric acid (2 M in diethyl ether, 0.300 mL, 0.600 mmol). After addition, the mixture was concentrated under reduced pressure. The resulting solid was triturated with methylene chloride and filtered to afford compound (**1 HCl**) as pale yellow solid: ¹H NMR (500 MHz, DMSO-*d*₆) δ 10.94 (s, 1H), 10.84 (bs, 1H), 10.22 (s, 1H), 7.75–6.90 (m, 6H), 4.49 (d, J = 14.5 Hz, 1H), 4.22–4.16 (m, 1H), 3.65–3.62 (m, 1H), 3.38–3.05 (m, 5H), 1.32 (t, J = 7.2 Hz, 3H); HRMS (ESI) m/z calculated for C₁₇H₁₉ClN₄O₂S [M + H]⁺ 379.09899, found 379.10085.

(±)-2-Amino-9-methyl-5,6,7,8-tetrahydro-4H-5,8-epiminocyclohepta[b]thiophene-3-carboxamide. The stirred mixture of tropinone (3.00 g, 21.6 mmol), 2-cyanoacetamide (1.99 g, 23.7 mmol), sulfur (830 mg, 25.9 mmol), and morpholine (3.75 g, 43.0 mmol) in ethanol (80 mL) was heated to reflux under nitrogen for 4 h. After this time, the reaction mixture was cooled to room temperature and concentrated under reduced pressure. The resulting residue was diluted with saturated aqueous sodium bicarbonate (60 mL) and extracted with methylene chloride (3 × 150 mL). The combined organic extracts were dried over anhydrous sodium sulfate, filtered, and concentrated under reduced pressure. The resulting residue was purified by flash column chromatography on silica gel eluting with methanol/methylene chloride (1:9) to provide compound (±)-2-amino-9-methyl-5,6,7,8-tetrahydro-4H-5,8-epiminocyclohepta[b]thiophene-3-carboxamide as a brown solid (396 mg, 8%): LRMS m/z 238 [M + H]⁺.

(±)-2-[3-(4-Chlorophenyl)ureido]-9-methyl-5,6,7,8-tetrahydro-4H-5,8-epiminocyclohepta[b]thiophene-3-carboxamide (88). To the stirred mixture of 2-amino-9-methyl-5,6,7,8-tetrahydro-4H-5,8-epiminocyclohepta[b]thiophene-3-carboxamide (375 mg, 1.58 mmol) in methylene chloride (10 mL) at room temperature under nitrogen was added a solution of 4-chlorophenyl isocyanate (255 mg, 1.66 mmol) in methylene chloride (10 mL). The reaction mixture was stirred overnight and concentrated under reduced pressure. The resulting residue was purified by flash column chromatography on silica gel eluting with methanol/methylene chloride (15:85) to provide compound **88** as an off-white solid (369 mg, 60%): ¹H NMR (300 MHz, DMSO-*d*₆) δ 10.70 (bs, 1H), 10.05 (bs, 1H), 7.90–6.50 (m, 6H), 4.11 (bs, 1H), 2.99 (d, J = 14.1 Hz, 1H), 2.35–1.95 (m, 7H), 1.79 (bs, 1H), 1.48 (bs, 1H); LRMS m/z 391 [M + H]⁺.

(–)-2-[3-(4-Chlorophenyl)ureido]-9-methyl-5,6,7,8-tetrahydro-4H-5,8-epiminocyclohepta[b]thiophene-3-carboxamide (89) and (+)-2-[3-(4-Chlorophenyl)ureido]-9-methyl-5,6,7,8-tetrahydro-4H-5,8-epiminocyclohepta[b]thiophene-3-carboxamide (90). Compound **88** (720 mg) was separated by chiral preparative HPLC (20 μ m CHIRALCEL OD, 5 cm × 50 cm, 100 mL/min flow rate, 120 mg/injection) eluting with 0.1% diethylamine in 20% ethanol/heptane to provide **89** (268 mg, 37%) as a white solid, LRMS m/z 391 [M + H]⁺, followed by **90** (250 mg, 35%) as a white solid. LRMS m/z 391 [M + H]⁺. Free base optical rotations: **89**, –19.5° (c = 0.2, MeOH), T = 25 °C; **90**, +18.5° (c = 0.2, MeOH), T = 25 °C.

(–)-2-[3-(4-Chlorophenyl)ureido]-9-methyl-5,6,7,8-tetrahydro-4H-5,8-epiminocyclohepta[b]thiophene-3-carboxamide Hydrochloride (89-HCl). To the stirred mixture of compound **89** (free base) (240 mg, 0.610 mmol) in methanol (30 mL) at room temperature was added 1 M hydrochloric acid (1.25 mL, 1.25 mmol) dropwise. After addition, the mixture was stirred for 10 min. After this time, the mixture was diluted with water (10 mL) and

lyophilized to provide compound **89** as a white solid (255 mg, 97%): $^1\text{H NMR}$ (300 MHz, $\text{DMSO}-d_6$) δ 11.24 (bs, 0.40 H), 10.34 and 10.32 (2 s, 1H), 10.19–10.16 (m, 1.60H), 7.51–7.48 (m, 4H), 7.35 (d, $J = 9.0$ Hz, 2H), 4.95–4.82 (m, 1H), 4.19–4.08 (m, 1H), 3.43–3.17 (m, 1H), 2.88–2.68 (m, 4H), 2.45–2.09 (m, 3H), 1.89–1.80 (m, 1H); optical rotation $[\alpha]_D = -5.5^\circ$ ($c = 0.2$, MeOH); HRMS (ESI) m/z calculated for $\text{C}_{18}\text{H}_{19}\text{ClN}_4\text{O}_2\text{S}$ $[\text{M} + \text{H}]^+$ 391.09899, found 391.09906.

(+)-2-[3-(4-Chlorophenyl)ureido]-9-methyl-5,6,7,8-tetrahydro-4H-5,8-epiminocyclohepta[b]thiophene-3-carboxamide Hydrochloride (**90-HCl**). To the stirred mixture of compound **90** (free base) (220 mg, 0.60 mmol) in methanol (30 mL) at room temperature was added 1 M hydrochloric acid (1.25 mL, 1.25 mmol) dropwise. After addition, the mixture was stirred for 10 min. After this time, the mixture was diluted with water (10 mL) and lyophilized to provide compound **90** as a white solid (243 mg, 96%): $^1\text{H NMR}$ (300 MHz, $\text{DMSO}-d_6$) δ 11.20 (bs, 0.34H), 10.34 and 10.31 (2 s, 1H), 10.18 (s, 1H), 10.16 (bs, 0.66H), 7.54–7.33 (m, 6H), 4.94–4.90 (m, 1H), 4.20–4.06 (m, 1H), 3.42–3.16 (m, 1H), 2.88–2.65 (m, 4H), 2.49–2.28 (m, 2H), 2.21–2.09 (m, 1H), 1.89–1.80 (m, 1H); optical rotation $[\alpha]_D = +3.5^\circ$ ($c = 0.2$, MeOH); HRMS (ESI) m/z calculated for $\text{C}_{18}\text{H}_{19}\text{ClN}_4\text{O}_2\text{S}$ $[\text{M} + \text{H}]^+$ 391.09899, found 391.09907.

■ ASSOCIATED CONTENT

● Supporting Information

(PDF) (CSV) The Supporting Information is available free of charge on the ACS Publications website at DOI: 10.1021/acs.jmedchem.7b00932.

Reproducibility of zebrafish lateral line hair cells viability assay, pharmacokinetic and toxicological properties of **90**, compound **90** crystal structure determination, non-interference in antimicrobial activity of aminoglycoside antibiotics, full experimental procedures, and characterization of compounds **1–99** (PDF)

SMILES strings for reported compounds (CSV)

Accession Codes

X-ray crystallographic structure of **90 HCl** has been deposited at The Cambridge Crystallographic Database (CSD) with the accession code CCDC-1557948 (<http://ccdc.cam.ac.uk>).

■ AUTHOR INFORMATION

Corresponding Author

*Phone: 206-667-6241. Fax: 206-667-5255. E-mail: jsimon@fredhutch.org

ORCID

Julian A. Simon: 0000-0001-9235-7565

Notes

The authors declare the following competing financial interest(s): Part of the research reported was funded by Oricula Therapeutics. G.J., V.E.G., D.W.R., E.W.R., and J.A.S. are founders of Oricula Therapeutics.

■ ACKNOWLEDGMENTS

We thank AMRI chemistry colleagues Randall Davis and Feryan Ahmed for synthetic efforts in support of this program. We also thank Dr. Brandon Mercado of the Yale University Chemical and Biophysical Instrumentation Center for X-ray crystal structure determination of **90 HCl**. We are also grateful for the assistance of Kelly Owens, Allison Hixon, Divya Mehta, Heather Kinnear, and Patricia Wu for carrying out the zebrafish assays and to Carol Robbins, Brianna Moore, Robin Gibson, and Van Redilia for carrying out the mammalian ABR studies. Tor Linbo and Glen MacDonald provided invaluable technical assistance, and David White provided excellent maintenance

and breeding advice in the zebrafish facility. We gratefully acknowledge the contributions of Jill Heemskerk, Nancy Freeman, and Charles Cywin (National Institutes of Health program staff). The research described here was supported by the grants U01NS074506, RO1DC013688, R01DC05987, and RO1DC009807 from the National Institutes of Health and funds from Washington State Life Sciences Discovery Fund.

■ ABBREVIATIONS USED

ADME, absorption, distribution, metabolism, and excretion; AGAs, aminoglycoside antibiotics; dpf, days post fertilization; hERG, human ether-à-go-go-related gene; ABR, auditory brain stem response; DASPEI, 2-[4-(dimethylamino)styryl]-N-ethylpyridinium iodide; TEA, triethylamine; THF, tetrahydrofuran

■ REFERENCES

- (1) Parham, K.; McKinnon, B. J.; Eibling, D.; Gates, G. A. Challenges and Opportunities in Presbycusis. *Otolaryngol.–Head Neck Surg.* **2011**, *144*, 491–495.
- (2) Mohr, P. E.; Feldman, J. J.; Dunbar, J. L. The Societal Costs of Severe to Profound Hearing Loss in the United States. *Policy Anal. Brief H Ser.* **2000**, *2*, 1–4.
- (3) Wong, A. C.; Ryan, A. F. Mechanisms of Sensorineural Cell Damage, Death and Survival in the Cochlea. *Front. Aging Neurosci.* **2015**, *7*, 58.
- (4) Rubel, E. W.; Furrer, S. A.; Stone, J. S. A Brief History of Hair Cell Regeneration Research and Speculations on the Future. *Hear. Res.* **2013**, *297*, 42–51.
- (5) Cunningham, L. L.; Cheng, A. G.; Rubel, E. W. Caspase Activation in Hair Cells of the Mouse Utricle Exposed to Neomycin. *J. Neurosci.* **2002**, *22*, 8532–8540.
- (6) Jiang, H.; Sha, S. H.; Schacht, J. Kanamycin Alters Cytoplasmic and Nuclear Phosphoinositide Signaling in the Organ of Corti in Vivo. *J. Neurochem.* **2006**, *99*, 269–276.
- (7) Op de Beeck, K.; Schacht, J.; Van Camp, G. Apoptosis in Acquired and Genetic Hearing Impairment: The Programmed Death of the Hair Cell. *Hear. Res.* **2011**, *281*, 18–27.
- (8) Wang, J.; Van De Water, T. R.; Bonny, C.; de Ribaupierre, F.; Puel, J. L.; Zine, A. A Peptide Inhibitor of C-Jun N-Terminal Kinase Protects against Both Aminoglycoside and Acoustic Trauma-Induced Auditory Hair Cell Death and Hearing Loss. *J. Neurosci.* **2003**, *23*, 8596–8607.
- (9) Battin, E. E.; Brumaghim, J. L. Antioxidant Activity of Sulfur and Selenium: A Review of Reactive Oxygen Species Scavenging, Glutathione Peroxidase, and Metal-Binding Antioxidant Mechanisms. *Cell Biochem. Biophys.* **2009**, *55*, 1–23.
- (10) Schacht, J.; Talaska, A. E.; Rybak, L. P. Cisplatin and Aminoglycoside Antibiotics: Hearing Loss and Its Prevention. *Anat. Rec.* **2012**, *295*, 1837–1850.
- (11) Rizzi, M. D.; Hirose, K. Aminoglycoside Ototoxicity. *Curr. Opin. Otolaryngol. Head Neck Surg.* **2007**, *15*, 352–357.
- (12) Le, T. N.; Straatman, L. V.; Lea, J.; Westerberg, B. Current Insights in Noise-Induced Hearing Loss: A Literature Review of the Underlying Mechanism, Pathophysiology, Asymmetry, and Management Options. *J. Otolaryngol. Head Neck Surg.* **2017**, *46*, 41.
- (13) Bagger-Sjoberg, D.; Stromback, K.; Hakizimana, P.; Plue, J.; Larsson, C.; Hultcrantz, M.; Papatziamos, G.; Smeds, H.; Danckwardt-Lilliestrom, N.; Hellstrom, S.; Johansson, A.; Tideholm, B.; Fridberger, A. A Randomised, Double Blind Trial of N-Acetylcysteine for Hearing Protection During Stapes Surgery. *PLoS One* **2015**, *10*, e0115657.
- (14) Pirvola, U.; Xing-Qun, L.; Virkkala, J.; Saarna, M.; Murakata, C.; Camoratto, A. M.; Walton, K. M.; Ylikoski, J. Rescue of Hearing, Auditory Hair Cells, and Neurons by Cep-1347/Kt7515, an Inhibitor of C-Jun N-Terminal Kinase Activation. *J. Neurosci.* **2000**, *20*, 43–50.
- (15) Ylikoski, J.; Xing-Qun, L.; Virkkala, J.; Pirvola, U. Blockade of C-Jun N-Terminal Kinase Pathway Attenuates Gentamicin-Induced Cochlear and Vestibular Hair Cell Death. *Hear. Res.* **2002**, *163*, 71–81.

- (16) Bodmer, D.; Brors, D.; Pak, K.; Gloddek, B.; Ryan, A. Rescue of Auditory Hair Cells from Aminoglycoside Toxicity by Clostridium Difficile Toxin B, an Inhibitor of the Small Gtpases Rho/Rac/Cdc42. *Hear. Res.* **2002**, *172*, 81–86.
- (17) Eshraghi, A. A.; Wang, J.; Adil, E.; He, J.; Zine, A.; Bublik, M.; Bonny, C.; Puel, J. L.; Balkany, T. J.; Van De Water, T. R. Blocking C-Jun-N-Terminal Kinase Signaling Can Prevent Hearing Loss Induced by Both Electrode Insertion Trauma and Neomycin Ototoxicity. *Hear. Res.* **2007**, *226*, 168–177.
- (18) Sugahara, K.; Rubel, E. W.; Cunningham, L. L. Jnk Signaling in Neomycin-Induced Vestibular Hair Cell Death. *Hear. Res.* **2006**, *221*, 128–135.
- (19) Sagwa, E. L.; Ruswa, N.; Mavhunga, F.; Rennie, T.; Leufkens, H. G.; Mantel-Teeuwisse, A. K. Comparing Amikacin and Kanamycin-Induced Hearing Loss in Multidrug-Resistant Tuberculosis Treatment under Programmatic Conditions in a Namibian Retrospective Cohort. *BMC Pharmacol. Toxicol.* **2015**, *16*, 36.
- (20) Harris, T.; Peer, S.; Fagan, J. J. Audiological Monitoring for Ototoxic Tuberculosis, Human Immunodeficiency Virus and Cancer Therapies in a Developing World Setting. *J. Laryngol. Otol.* **2012**, *126*, 548–551.
- (21) Lawson, L.; Yassin, M. A.; Abdurrahman, S. T.; Parry, C. M.; Dacombe, R.; Sogaolu, O. M.; Ebisike, J. N.; Uzoewulu, G. N.; Lawson, L. O.; Emenyonu, N.; Ouoha, J. O.; David, J. S.; Davies, P. D.; Cuevas, L. E. Resistance to First-Line Tuberculosis Drugs in Three Cities of Nigeria. *Trop. Med. Int. Health* **2011**, *16*, 974–980.
- (22) Garinis, A. C.; Cross, C. P.; Srikanth, P.; Carroll, K.; Feeney, M. P.; Keefe, D. H.; Hunter, L. L.; Putterman, D. B.; Cohen, D. M.; Gold, J. A.; Steyger, P. S. The Cumulative Effects of Intravenous Antibiotic Treatments on Hearing in Patients with Cystic Fibrosis. *J. Cystic Fibrosis* **2017**, *16*, 401–409.
- (23) Skolnik, K.; Kirkpatrick, G.; Quon, B. S. Nontuberculous Mycobacteria in Cystic Fibrosis. *Curr. Treat. Options Infect. Dis.* **2016**, *8*, 259–274.
- (24) Lee, B. Y.; Clemens, D. L.; Silva, A.; Dillon, B. J.; Maslesa-Galic, S.; Nava, S.; Ding, X.; Ho, C. M.; Horwitz, M. A. Drug Regimens Identified and Optimized by Output-Driven Platform Markedly Reduce Tuberculosis Treatment Time. *Nat. Commun.* **2017**, *8*, 14183.
- (25) Mayer-Hamblett, N.; Kloster, M.; Rosenfeld, M.; Gibson, R. L.; Retsch-Bogart, G. Z.; Emerson, J.; Thompson, V.; Ramsey, B. W. Impact of Sustained Eradication of New Pseudomonas Aeruginosa Infection on Long-Term Outcomes in Cystic Fibrosis. *Clin. Infect. Dis.* **2015**, *61*, 707–715.
- (26) Lando, D.; Cousin, M. A.; Privat de Garilhe, M. Misreading, a Fundamental Aspect of the Mechanism of Action of Several Aminoglycosides. *Biochemistry* **1973**, *12*, 4528–4533.
- (27) Goffic, F.; Capmau, M. L.; Tangy, F.; Baillarge, M. Mechanism of Action of Aminoglycoside Antibiotics. Binding Studies of Tobramycin and Its 6'-N-Acetyl Derivative to the Bacterial Ribosome and Its Subunits. *Eur. J. Biochem.* **1979**, *102*, 73–81.
- (28) Yoshizawa, S.; Fourmy, D.; Puglisi, J. D. Structural Origins of Gentamicin Antibiotic Action. *EMBO J.* **1998**, *17*, 6437–6448.
- (29) Brodersen, D. E.; Clemons, W. M., Jr.; Carter, A. P.; Morgan-Warren, R. J.; Wimberly, B. T.; Ramakrishnan, V. The Structural Basis for the Action of the Antibiotics Tetracycline, Pactamycin, and Hygromycin B on the 30s Ribosomal Subunit. *Cell* **2000**, *103*, 1143–1154.
- (30) Kohanski, M. A.; Dwyer, D. J.; Hayete, B.; Lawrence, C. A.; Collins, J. J. A Common Mechanism of Cellular Death Induced by Bactericidal Antibiotics. *Cell* **2007**, *130*, 797–810.
- (31) Foti, J. J.; Devadoss, B.; Winkler, J. A.; Collins, J. J.; Walker, G. C. Oxidation of the Guanine Nucleotide Pool Underlies Cell Death by Bactericidal Antibiotics. *Science* **2012**, *336*, 315–319.
- (32) Kalghatgi, S.; Spina, C. S.; Costello, J. C.; Liesa, M.; Morones-Ramirez, J. R.; Slomovic, S.; Molina, A.; Shirihai, O. S.; Collins, J. J. Bactericidal Antibiotics Induce Mitochondrial Dysfunction and Oxidative Damage in Mammalian Cells. *Sci. Transl. Med.* **2013**, *5*, 192ra185.
- (33) Karasawa, T.; Wang, Q.; David, L. L.; Steyger, P. S. Climp-63 Is a Gentamicin-Binding Protein That Is Involved in Drug-Induced Cytotoxicity. *Cell Death Dis.* **2010**, *1*, e102.
- (34) Owens, K. N.; Santos, F.; Roberts, B.; Linbo, T.; Coffin, A. B.; Knisely, A. J.; Simon, J. A.; Rubel, E. W.; Raible, D. W. Identification of Genetic and Chemical Modulators of Zebrafish Mechanosensory Hair Cell Death. *PLoS Genet.* **2008**, *4*, e1000020.
- (35) Brown, A. M. Herg Block, Qt Liability and Sudden Cardiac Death. *Novartis Found. Symp.* **2005**, *266*, 118–131.
- (36) Taboureau, O.; Jorgensen, F. S. In Silico Predictions of Herg Channel Blockers in Drug Discovery: From Ligand-Based and Target-Based Approaches to Systems Chemical Biology. *Comb. Chem. High Throughput Screening* **2011**, *14*, 375–387.
- (37) Vandenberg, J. I.; Perry, M. D.; Perrin, M. J.; Mann, S. A.; Ke, Y.; Hill, A. P. Herg K(+) Channels: Structure, Function, and Clinical Significance. *Physiol. Rev.* **2012**, *92*, 1393–1478.
- (38) Witchel, H. J. Drug-Induced Herg Block and Long Qt Syndrome. *Cardiovasc. Ther.* **2011**, *29*, 251–259.
- (39) Eggert, U. S. The Why and How of Phenotypic Small-Molecule Screens. *Nat. Chem. Biol.* **2013**, *9*, 206–209.
- (40) Wagner, B. K.; Schreiber, S. L. The Power of Sophisticated Phenotypic Screening and Modern Mechanism-of-Action Methods. *Cell Chem. Biol.* **2016**, *23*, 3–9.
- (41) Eller, G. A.; Holzer, W. First Synthesis of 3-Acetyl-2-Aminothiophenes Using the Gewald Reaction. *Molecules* **2006**, *11*, 371–376.
- (42) Huang, Y.; Domling, A. The Gewald Multicomponent Reaction. *Mol. Diversity* **2011**, *15*, 3–33.
- (43) Coffin, A. B.; Rubel, E. W.; Raible, D. W. Bax, Bcl2, and P53 Differentially Regulate Neomycin- and Gentamicin-Induced Hair Cell Death in the Zebrafish Lateral Line. *J. Assoc. Res. Otolaryngol.* **2013**, *14*, 645–659.
- (44) Simon, J. A.; Johnson, G.; Rubel, E.; Raible, D. W.; Gonzales, M. D.; Metzler, P. C.; Miao, W. Compound and Methods for Preventing or Treating Sensory Hair Cell Death. U.S. Patent 9,493,482, 2016.
- (45) Cheng, A. G.; Cunningham, L. L.; Rubel, E. W. Mechanisms of Hair Cell Death and Protection. *Curr. Opin. Otolaryngol. Head. Neck Surg.* **2005**, *13*, 343–348.
- (46) Harris, J. A.; Cheng, A. G.; Cunningham, L. L.; MacDonald, G.; Raible, D. W.; Rubel, E. W. Neomycin-Induced Hair Cell Death and Rapid Regeneration in the Lateral Line of Zebrafish (Danio Rerio). *J. Assoc. Res. Otolaryngol.* **2003**, *4*, 219–234.
- (47) Raible, D. W.; Kruse, G. J. Organization of the Lateral Line System in Embryonic Zebrafish. *J. Comp. Neurol.* **2000**, *421*, 189–198.